

AD-A090 549

STANFORD UNIV CALIF DEPT OF PHYSICS  
FUNDAMENTAL EXPERIMENT AT LIQUID HELIUM TEMPERATURE.(U)  
SEP 79

F/6 20/7

F44620-75-C-0022

UNCLASSIFIED

AFOSR-TR-80-1009

NL

[ ] [ ]  
AD-  
ADDRESS



END  
DATE  
FILMED  
11 80  
DTIC

6 FUNDAMENTAL EXPERIMENT AT LIQUID  
HELIUM TEMPERATURE.

AFOSR/TR-80-1009

INTRODUCTION

LEVEL III

A012919

FINAL

12

This document constitutes the Final Report for Air Force Contract  
F44620-75-C-0022, Fundamental Experiments at Liquid Helium Temperature,  
October 1, 1974 to September 31, 1979. Our purpose in this report is to  
summarize the research undertaken during this period, identifying the  
research topics and the principal results obtained. A detailed summary  
of our research is provided in the attached appendices.

AD A090549

Final report on 4-31-1980

DTIC  
ELECTE  
OCT 17 1980

C

31

14

DDC FILE COPY

80 10 3 100

Approved for public release;  
distribution unlimited.

3 2 1 7

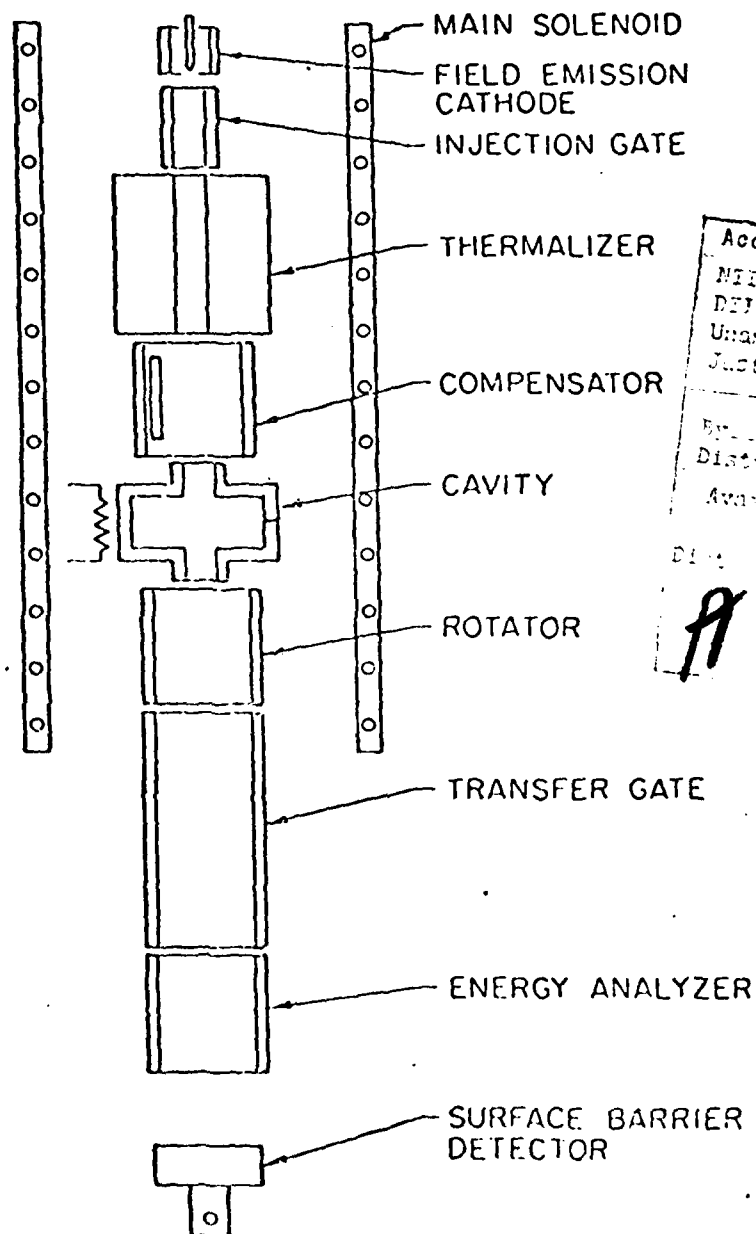


Fig. 1. A schematic diagram of the electron thermalizer apparatus.

The spread in energy of the bunch is a few eV and the cathode is biased to maximize the number of electrons entering the trap with  $p_z \approx 0$ . The injection gate is closed just before the end of the cathode pulse.

The walls of the thermalizer section are made of a resistive material to which the trapped electrons can transfer their kinetic energy through induced eddy currents. Thermalization of the cyclotron levels is enhanced by including a TE mode microwave cavity tuned to the cyclotron resonance within the trap. The electrons in the magnetic field in the cavity form a coupled oscillator system in which energy transfer from the electrons to the cavity walls is enhanced in proportion to the Q of the cavity. The thermalization time to 4 K for the z-momentum is calculated to be about 80 msec.

Following thermalization of  $p_z$ , the trapping potentials are changed to restrict the electrons to the center section of the trap to decouple them from the thermalizer. The transfer gate is then lowered to permit all but the ground state electrons to escape. At the end of the cycle the remaining ground state electrons are run through an electro-static energy analyzer to measure the spectrum.

Slow Positron Source: To adapt the thermalizer for use as a positron source the field emission cathode will be replaced by a positron emitter. The positron energy can be reduced to a few eV through inelastic scattering within a solid absorber<sup>3,4</sup> and the moderated positrons can be trapped and thermalized to 4 K as described above. Adiabatic expansion<sup>5</sup> can be used to reduce the thermalized positron energy from  $\sim 10^{-4}$  eV at 4 K to below  $10^{-7}$  eV for use in the gravitational experiments.

Stabilization: The principal experimental complication with this setup is the diffusion of the trapped electrons across the magnetic field lines due to stray transverse electric fields and curvature of the magnetic field lines.

The drift due to a uniform transverse electric field of B-field gradient can be suppressed by rotating the electron distribution about the axis at a rate rapid in comparison to the time required to drift across the trap. In the present apparatus this is accomplished during passage of the trapped electrons between the cavity and the rotator section (see Figure 2). A similar technique has been used by Dehmelt.<sup>6</sup> However, if the average  $(\underline{E} \times \underline{B}/B^2)$  or  $(V|\underline{B}| \times \underline{B})/B^2$  drift has a transverse gradient, the rotation of the distribution can result in either exponential radial expansion or contraction of the distribution, depending on the direction of the gradient. To suppress this effect, a compensating element has been added to the apparatus to permit the introduction of a transverse electric field with a controlled gradient. This element is used to cancel the average transverse gradient to which the electrons are exposed during their passage through the rest of the trap.

#### Experimental Performance of the Prototype

One of the most serious problems has been in the selection of a suitable material for the thermalizer section of the apparatus. A carbon-glass material was used, but problems were encountered with the surface potential variations, and in obtaining a mixture which would have a suitable resistivity. Trapping lifetimes in excess of 700 msec for 100 meV electrons and 150 msec for electrons with energies below 100 meV have been achieved when the carbon-glass thermalizer was removed from the system. The 700 msec trapping time appears to be more than needed for the thermalization process. We suspect that the more rapid decay of the low energy portion of the distribution can be improved by increasing the rotation rate of the beam about the axis of the apparatus to more effectively average over stray fields.

However, typical decay rates in the experiments using the eddy-current system were of the order of 20 to 40 msec. It was possible to increase these values somewhat by applying a relatively large transverse electric field.

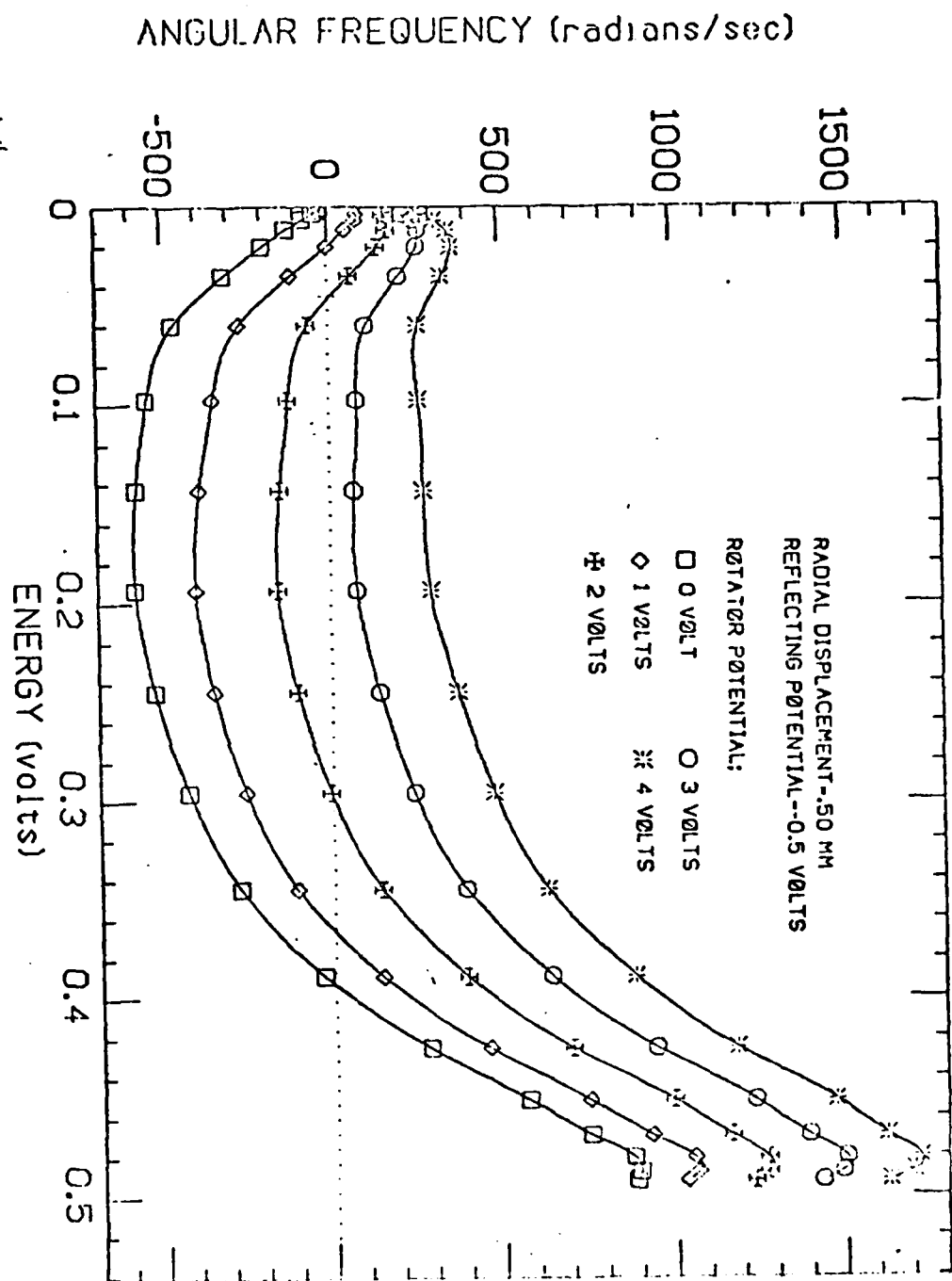


Figure 2. Rotation rate of electrons about axis verse electron energy.

presumably cancels the electric field due to variations in the electrostatic potential over the surface of the thermalizer. Attempts to smooth out the potential variations by coating the surface with a thin layer of graphite were unsuccessful.

We are now experimenting with making the thermalizer out of silicon. The resistance of silicon, even doped silicon, is high at 4°K but it can be lowered through photogeneration of electrical carriers. We have shown that a resistance of 50  $\Omega$ -cm at 4°K can be obtained with 20-100 mW of 1  $\mu$ m light. Pure grade single crystal silicon is available and should have small surface potential variations.

One difficulty which has to be overcome is that of maintaining electrical contact with the material at low temperatures. Evaporation methods failed to yield ohmic contacts, making measurements of the bulk resistance impossible. By using an ion implantation process, followed by laser annealing, we were able to get surface carrier concentrations of  $5 \times 10^{15}/\text{cm}^2$ . The ion-implanted terminals remain ohmic to below 4° K.

## REFERENCES

1. Lockhart, J. M., Witteborn, F. C., and Fairbank, W. M., Phys. Rev. Lett. 38 (1977) 1220.
2. Bloch, F., Physica 19 (1953) 821.
3. Madey, J. M. J., Phys. Rev. Lett. 22 (1969) 784.
4. McGowan, J. W., The Physics of Electronic and Atomic Collisions, edited by Govers, T. R. and DeHeer, F. J., (North-Holland Publishing Company, Amsterdam) 1972.
5. Witteborn, F. C. and Fairbank, W. M., Nature 220 (1968) 436.
6. Wineland, D. J. and Dehmelt, H. G., Journ. Appl. Phys. 46 (1975) 919.



## APPENDIX A.2: Status of Electron/Positron Thermalizer:

A source of low energy positrons would be useful to clarify the nature of the anomalous surface shielding effects observed in the copper drift tubes of earlier experiments.<sup>1</sup> Positron sources have been constructed which give an energy distribution with a width of  $\sim 1$  eV. What is needed is a method of further lowering the energy of a few of the positrons to  $\sim 10^{-7}$  eV. The prototype source which we have been investigating is designed to confine an electron distribution with  $\sim 1$  eV width and thermalize it to  $\sim 10^{-4}$  eV ( $\sim 4^\circ\text{K}$ ). Adiabatic expansion will then be used to reduce the width to  $\sim 10^{-6}$  eV. The following section contains a description of the device built and its performance to date.

Description of Operation: The energy of a non-relativistic free electron moving in a homogeneous magnetic field in the  $z$  direction is given by:<sup>2</sup>

$$E_{n,s} = p_z^2/2m + (2n + 1 + g_e m_s) B \mu_0$$

where  $B$  is the magnetic field,  $m$  is the electron mass,  $\mu_0$  is the Bohr magneton,  $n$  is the cyclotron number,  $g_e$  ( $g$ -factor) is  $\sim 2.0023$ ,  $m_s$  is the spin quantum number ( $\pm 1/2$ ), and  $p_z$  is the  $z$ -momentum. The fact that only the magnetic ground state ( $n = 0$ ,  $m_s = -1/2$ ) has a negative magnetic energy permits the device to distinguish electrons in the ground state from those in higher magnetic states.

A schematic of the device is shown in Figure 1. To a first approximation the axial magnetic field constrains the electrons to move along the axis. Trapping is accomplished by applying appropriate electric potentials to the cylindrical electrodes. During the first step the injection gate is lowered to allow entry of a low current electron beam from a field-emission cathode.

## SUMMARY:

Our research during the past five years has been concentrated in six basic areas: 1) the analysis of the forces acting on ultra-low energy electrons in the electron-positron free-fall experiment and the determination of the properties of the surface state on copper at low temperatures, 2) the determination of the properties of polarized  $\text{He}^3$  at low temperatures, 3) the development of ultra-sensitive low temperature techniques to measure the susceptibility of water and room-temperature organic molecules, 4) the analysis and development of an ultra-sensitive accelerometer for use in the detection of gravitational radiation, 5) studies of local and non-local effects in superconducting thin films, and 6) the use of superconducting SQUID magnetometers to measure the electrical activity of the heart.

### Forces on Low Energy Electrons, and the Surface State of Copper:

For several years, experiments have been conducted with Air Force support to measure the force of gravity on single electrons and positrons using cryogenic techniques (Appendices A1-A6). In the course of this work it was found that the ambient electric field along the axis of copper shielding tubes used in the electron time-of-flight measurements was several orders of magnitude smaller than expected. Two contributions to the tube's ambient axial electric field are expected: a spatially fluctuating potential of rms amplitude  $10^{-6}$  V caused by the patch effect (contact potential differences between adjacent crystalline metal) and a constant electric field of about  $10^{-6}$  V/m due to gravitationally-induced differential compression of the tube's ionic lattice. The axis of the tube was shown to be shielded from these fields by at least a factor of  $10^5$  (Appendix A1). Further experiments at room temperature (in contrast to the 4.2 K temperature of the earlier work) indicated that this form of shielding was not present at

(Appendix A2).

In an effort to understand these results, a set of experiments was performed in which the ambient axial electric field in the tube was measured at temperatures ranging from 4.2 K to 77 K. These measurements resulted in the discovery of the sudden transition in the shielding effect at 4.5 K (Appendices A4, A5 and A6).

While the experimental work on this problem is continuing, we have also sought to review the possible theoretical explanations for the phenomenon. Our objective was to determine what could be said theoretically about the shielding on the basis of what is known about the surface of the drift tubes used in the experiment. While very little is in fact known about the surface, it is possible to reach a number of fundamental conclusions on the basis of an order of magnitude estimate of the surface electron density, the surface layer thickness, and the statistics of the surface electrons.

We have, in particular, explored the possibility that the shielding results from a two-dimensional electron layer just outside the copper oxide whose electrons (of density  $10^{11}$  to  $10^{12}$  per square centimeter) are supplied from the copper via tunnelling through the copper oxide. In this theory the transition to a nearly perfect shielding state is the result of a Bose-Einstein condensation of electron hole pairs (Appendices A7 and A8).

We found that the electric field at the surface could be equated to the sum of  $mg/e$  plus  $\partial\mu/\partial z$ . The quantity  $mg/e$  is the original Schiff-Barnhill field and is the field seen in the 4 K free-fall experiment. The quantity  $\partial\mu/\partial z$  is the gradient of the chemical potential of the surface electrons and depends on the number density and statistics. If Fermi statistics are assumed,  $\partial\mu/\partial z$  is  $10^5$  times larger than  $mg/e$  at 4 K, a result incompatible with the experiment. With Bose statistics,  $\partial\mu/\partial z$  approaches zero at low

superconducting shields. A crude prototype of a cryogenic  $\text{He}^3$  gyroscope was built and tested inside such a shield. The  $\text{He}^3$  was polarized by optical pumping mixed with  $\text{He}^4$  and condensed into a 4° k Pyrex bulb using the superconducting shield. The resulting processing magnetization was observed with a signal-to-noise ratio in excess of  $10^3$  by use of a SQUID magnetometer. Although this prototype was too flawed (in large part due to magnetic contaminants) to function as a gyro, it was found that 0.07%  $\text{He}^3$ -liquid  $\text{He}^4$  mixture had a relaxation time of 40 hours in a 1 cm diameter Pyrex cell when the effect of magnetic-gradient-induced relaxation was deducted. This result was dominated by wall-induced relaxation since the subsequent use of a solid  $\text{H}_2$  wall coating increased this relaxation time to more than five days (140 hours). This last result is encouragingly close to the theoretically estimated maximum relaxation time under these conditions of 170 hours due to  $\text{He}^3$  -  $\text{He}^3$  dipolar interactions.

In addition to these experimental measurements, a general analysis of the characteristics of a  $\text{He}^3$  NG based on current low-temperature technology was made for the purpose of evaluating its potential for use in a future nuclear electric dipole moment experiment. This analysis considered two possible modes of operation of the  $\text{He}^3$  NG and the results of one of these analyses are presented in Section II. The details of both the theoretical analyses and the relaxation time measurements can be found in the Ph.D. thesis of M. A. Taber. A summary of the experimental results was also presented at the 15th International Conference on Low Temperature Physics and published in the Proceedings (Appendix B2, A2).

temperatures, and a transition temperature compatible with the experiment can be obtained with a plausible surface electron density.

The significance of this work lies in the conclusion that the shielding data cannot be explained if we assume the surface electrons follow Fermi statistics. Therefore something quite unique is going on on the surface of the copper drift tubes. The success of the ideal Bose model is tantalizing, but it remains to be determined why Bose statistics should govern the distribution of the surface electrons at low temperatures.

To further explore the nature of the shielding seen in copper in the free-fall experiment we have performed a number of experiments with an X-band copper microwave cavity. We have found a sudden small change in the frequency and Q at 3.7 K which, together with the observed magnetic field dependence and hysteresis, suggests superconductivity. These experiments are discussed more fully in Appendix A9. The experiments have revealed a number of fascinating effects, including transitions in the real and reactive components of the microwave surface impedance, and hysteretic behavior in the presence of a magnetic field. The experiments are discussed in further detail in Appendix A.9.

#### The Determination of the Properties of Polarized He<sup>3</sup> at Low Temperatures

We have conducted a series of experiments to determine the usefulness of polarized He<sup>3</sup> as a low temperature nuclear gyroscope. This work led in 1978 to separate Air Force funding to develop a nuclear He<sup>3</sup> gyroscope. The background work, done under the sponsorship of the Air Force Grant which is the subject of this final report, is described in detail in the Ph.D. thesis of Mike Taber (Appendix B1) and the paper presented to L.T. 15 (62). The technique was developed for producing a low magnetic field region inside

The Development of Ultra-Sensitive Low Temperature Techniques to Measure the Susceptibility of Water and Organic Molecules at Room Temperature

As part of a general program to exploit the properties of superconducting magnets and shields and the extreme sensitivity of the SQUID magnetometer for measuring magnetic fields, we developed under partial support from AFOSR a susceptometer capable of measuring the susceptibility of a room temperature sample to a sensitivity  $10^{-6}$  of the diamagnetism of water. With this apparatus, we measured with extreme accuracy the temperature dependence of the diamagnetism of water and showed that certain anomalies observed in other experiments were in reality not present.

We have developed a technique of measuring the magnetic changes in fast reactions in solution. The changes in magnetic susceptibility during the recombination reactions of hemoglobin with carbon monoxide after flash photolysis with measured time resolution of 1 ms. The susceptometer was more than 1 order of magnitude more sensitive than other existing susceptometers. The results of these experiments are described in Appendices C1, C2 and C3.

The Analysis and Development of an Ultra-Sensitive Accelerometer for Use in the Detection of Gravitational Radiation

In cooperation with NSF, a very sensitive resonant superconducting accelerometer to be used as a component of a cryogenic gravitational radiation detector was developed. The device consists of a superconducting test mass and superconducting coils carrying a persistent current. The displacement of the test mass modulates the inductances of the coils and generates an a.c. magnetic field which is detected by a Josephson junction magnetometer. The restoring force provided by the magnetic field is used to tune the resonant frequency of the transducer. The device is being used as a very

crucial part of a gravitational radiation detector which at the present time is capable of detecting changes in the energy of a 5 ton aluminum bar equivalent in energy to  $kT$  where  $T$  is  $1.4 \times 10^{-2}k$ . At the present time this accelerometer has been developed into a very sensitive gradiometer under separate new support from AFOSR. The work on the accelerometer is described in Appendix D1 and D2.

#### Studies of Local and Non-Local Effects in Superconducting Thin Films

Under partial support from the AFOSR a SQUID magnetometer was used to measure the dependence of magnetic field penetration into superconducting thin films. This work showed distinctly that non-local effects exist, as would be expected from the Pippard and BCS theories. This work is described in the Ph.D. thesis of Edward G. Wilson, Appendix E1.

#### The Use of Superconducting SQUID Magnetometers to Measure the Electrical Activity of the Heart

In cooperation with NSF, a superconducting SQUID magnetometer was developed into an instrument to measure the magnetic activity of the heart. This work is described in Appendix F1, the Ph.D. thesis of John Wikswo.